Journal of Power Sources 201 (2012) 395–401

Contents lists available at SciVerse ScienceDirect

Journal of Power Sources

journal homepage: www.elsevier.com/locate/jpowsour

Dye-sensitized solar cells using ion-gel electrolytes for long-term stability☆

Jinsun Yoon[a,b], Doc ki Kang[a], Jongok Won[a,*], Jun-Young Park[b], Yong Soo Kang[c]

[a] Department of Chemistry, Sejong University, 98 Gunja, Gwangjin, Seoul 143-747, Republic of Korea
[b] Department of Nano Technology and Advanced Materials Engineering, Sejong University, 98 Gunja, Gwangjin, Seoul 143-747, Republic of Korea
[c] WCU Department of Energy Engineering, Hanyang University, 1 Haengdang, Seongdong, Seoul 133-791, Republic of Korea

ARTICLE INFO

Article history:
Received 11 September 2011
Received in revised form 2 November 2011
Accepted 3 November 2011
Available online 12 November 2011

Keywords:
Dye-sensitized solar cell
Ion-gel
Ionic liquid
Triblock copolymer
Dendron

ABSTRACT

Dye-sensitized solar cells (DSSCs) with quasi-solid ion-gel electrolytes are fabricated using a 1-propyl-3-methyl imidazolium iodide (PMII) with a small amount of poly(styrene-block-ethyleneoxide-block-styrene) (SEOS) triblock copolymer. The interaction between the PMII and SEOS changes the liquid state of PMII into a solid state, and the interactions between the imidazolium cation of PMII and the ethyleneoxide of SEOS are confirmed by an ab initio method. The phase change of the electrolyte from an ionic liquid to a quasi-solid ion-gel in a DSSC slightly increases the photoconversion efficiency, and the DSSC containing an ion-gel maintains 92% of its efficiency under more than 1440 h of operation, which is higher than that with the ionic liquid as an electrolyte (78%) in this system. The addition of dendrons as a barrier-forming co-adsorbent increases the short-circuit current density (J_{sc}) of the DSSC. Up to a 27% increase in the power conversion efficiency are achieved with the G5 dendron as the co-adsorbent. EIS and IPCE measurements show that the increase in J_{sc} is due to the suppression of recombination by the surface coverage of the TiO_2 particles. The photocurrent and the conversion efficiency for all DSSCs prepared with quasi-solid ion-gel electrolytes and dendron co-adsorbents are higher than those prepared with an ionic liquid.

1. Introduction

Dye-sensitized solar cells (DSSCs) have received tremendous attention as the next generation of solar cells due to their low production costs and reasonable energy conversion efficiency of more than 11% [1,2]. The principle of energy conversion in DSSCs is based on the injection of electrons from a photoexcited state of a dye that is attached to a mesoporous TiO_2 semiconductor into the conduction band of the semiconductor. The oxidized dyes can be reduced by a redox mediator (for example, I^-/I_3^-) present in the electrolyte located between two electrodes, which must also be re-reduced at the counter-electrode, making the photoelectrochemical cell regenerative. Because the common matrix for the redox mediator is a liquid organic solvent such as volatile acetonitrile, the packaging of liquid-electrolyte DSSCs requires perfect sealing to avoid leakage, evaporation of the solvent and contamination by impurities for practical usage [3].

Several attempts have been made to substitute liquid electrolytes with room-temperature ionic liquids (RTILs), which have negligible vapor pressure [4], but the leakage problem has not been overcome. Therefore, solid- or quasi-solid state electrolytes such as solid polymer electrolytes [5–10], polymer gel electrolytes [11–13], and organic hole-transport materials [3,14] have been studied to address the drawbacks of liquid electrolytes. However, the increased viscosity of the medium leads to low and limited redox mediator transport [15] and/or an insufficient penetration of the electrolyte into the nanoporous TiO_2 photoelectrode [16], which in turn leads to lower photovoltaic performance when compared to DSSCs assembled with liquid electrolytes [17]. From this point of view, we have focused on an ion-gel electrolyte based on RTILs possessing high ionic conductivity to minimize leakage and maintain the feasibility of liquid-phase redox mediator transport.

It is reported that some RTILs become gels with the addition of polymers [18] and provide reasonably strong mechanical strength; however, the addition of polymer increases the viscosity of the matrix, which affects redox mediator diffusion in DSSCs. In addition, large amounts of polymer in the electrolyte prevent deep penetration of the electrolyte into the mesoporous structure of the semiconductor layer, resulting in defect formation on the interfacial contact between the electrolyte and the dye-adsorbed semiconductor layer. Therefore, a new solid or quasi-solid electrolyte with

☆ This work was presented at the Hybrid and Organic Photovoltaics Conference (HOPV2010, May 23–27, 2010, Assisi, Italy) and 5th Aseanian Conference on DSSCs (August 25–28, 2010, Huangshan, China).

* Corresponding author. Tel.: +82 2 3408 3230; fax: +82 2 3408 4317.
E-mail address: jwon@sejong.ac.kr (J. Won).

0378-7753/$ – see front matter © 2011 Elsevier B.V. All rights reserved.
doi:10.1016/j.jpowsour.2011.11.012

improved conductivity is required. One candidate is a physical gel created by the self-assembly of triblock copolymers in RTIL, which can be achieved by the addition of a small amount of triblock copolymers [19,20].

In this work, we investigated the effect of ion-gel electrolytes formed by the simple addition of poly(styrene-block-ethylene oxide-block-styrene) (SEOS) triblock copolymer to 1-propyl-3-methylimidazolium iodide (PMII), which has been widely used in DSSCs due to its high conductivity. In addition, PMII is known to interact with poly(ethylene oxide) (PEO), which is the central polymer moiety of the SEOS triblock copolymer [21]. Compared to conventional polymer gels, which require 10–30 wt% polymer to form gels [18], much less triblock copolymer is required for ion-gel formation (ca. 5 wt%). This small amount of triblock copolymer maintains the high ionic conductivity of PMII and improves the penetration of the ion-gel electrolyte into the mesopores of the TiO_2 layer, which provides large interfacial contact area between the electrolyte and the dye. To improve the performance of DSSCs, a well-defined structural material, dendron, was used to form an insulating layer, which effectively shields the back electron transfer from the TiO_2 conduction band to I_3^- [22]. The effect was confirmed by photovoltaic characterization.

2. Experimental methods

2.1. Materials

PMII was purchased from C-TRI, and TiO_2 paste (20 nm, Ti-Nanoxide T/SP), *cis*-diisothiocyanato-bis(2,2′-bipyridyl-4,4′-dicarboxylato)ruthenium(II) bis(tetrabutylammonium) (N719 dye) and surlyn film (Meltonix 1170-25, film thickness of 25 μm) were purchased from Solaronix. Conductive fluorine-doped tin oxide (FTO) (TEC8, 8 Ω/□, 2.3 mm) were purchased from Filkington Co. Fifth-generation polyester hydroxyl acetylene bis(hydroxymethyl) propanoic acid dendrons (dendron), I_2, tert-butanol, H_2PtCl_6, Ti(IV) bis(ethyl acetoacetato)-diisopropoxide, iso-propyl alcohol (IPA), 1-methylbenzimidazole (1MB), I_2, n-butanol, and dichloromethane (MC) were purchased from Aldrich Co. Poly(styrene-b-ethyleneoxide-b-styrene)s (SEOS1, Mw = 48,600; SEOS2, Mw = 70,400) were purchased from Polymer Source, Inc. (Canada) and used as received. The PEO weight fractions (f_{EO}) of SEOS1 and SEOS2 were 60%, and 68.8%, respectively.

2.2. Fabrication

The photoelectrode was fabricated by spin-coating Ti(IV) bis(ethyl acetoacetato)-diisopropoxide solution (2 wt% in n-butanol) onto the FTO glass and heating at 450 °C for 30 min. Then a 10-μm-thick TiO_2 layer was deposited over the FTO glass using the doctor-blade method and successive sintering at 450 °C for 30 min using TiO_2 paste. The TiO_2 thin film was dipped in 0.3 mM N719 dye in mixed solvents (1:1 mole ratio of acetonitrile and *tert*-butanol) for 18 h at 30 °C. Then the residual dye solution was rinsed with acetonitrile and dried with N_2 gas. For the treatment of dendron, 100 μl of 0.3 mM dendron solution was dropped onto the top of the dye-dipped cell and dried at room temperature for one day. Then the residual dendron was rinsed with acetonitrile and dried with N_2 gas. The active area of the DSSC was 0.5 cm × 0.5 cm. The Pt counter electrodes were prepared by spin-coating H_2PtCl_6 solution (0.01 M in IPA) onto the conductive FTO glass and successively sintering at 450 °C for 30 min. The Pt counter electrode and the dye-anchored photoelectrode were then assembled into a sealed sandwich-type cell using surlyn film.

The ionic liquid electrolyte was prepared by dissolving the appropriate amount of PMII, I_2 and 1MB in MC to form a homogeneous solution. The mole ratio of PMII/I_2/1MB was optimized to be 12:0.5:1. Ion-gel electrolytes were fabricated by dissolving 5 wt% of SEOS1 or SEOS2 copolymer in PMII/I_2/1MB solution in MC. MC was removed by evaporation at room temperature for 24 h, followed by placing the solution in a vacuum oven at 40 °C until a constant weight was achieved [19]. SEOS1 and SEOS2 films were also prepared using the same procedure.

2.3. Characterization

The ionic conductivity of the ion-gel electrolytes was determined using a laboratory-made four-point probe conductivity cell connected to an impedance analyzer (IM6e, Zahner) [23]. The ionic conductivities (σ) of the ion-gels were calculated using the relation $\sigma = L/ZA$, where L is the thickness of the electrolyte (cm), Z is the impedance (Ω) and A is the effective area (cm^2). Wide-angle X-ray diffraction analysis (WAXD) was conducted with a Rigaku, D/MAX RINT 2000 high-resolution diffractometer using Ni-filtered Cu Kα radiation. The scanning angle was varied from 4 to 75° at a scanning rate of 5° min^{-1}. All spectra were measured at ambient temperature. The current–voltage characteristics of the DSSCs were performed under 1-sun illumination (AM 1.5G, 100 mW cm^{-2}) with a Newport (USA) solar simulator (300 W Xe source) and a Keithley 2400 source meter using a mask with an aperture area of 0.36 cm^2. Electrochemical impedance spectroscopy (EIS) was measured with a potentiostat in a frequency range of 100 mHz–1 MHz under forward bias (−0.62 V) in the dark. The cross-section of the cell was examined by field-emission scanning electron microscopy (FE-SEM) (Hitachi S-4700, Japan). IPCEs (PV Measurement Inc.) were measured using a halogen source for monochromatic light and a broadband bias light to approximate the illumination of 1 sun. Raman measurements of the samples were made using a backscattering geometry with a Jobin-Yvon LabRam HR fitted with a liquid-nitrogen-cooled CCD detector. The spectra were collected under ambient conditions using the 514.532-nm line of an argon-ion laser (0.5 mW).

2.4. Computational method

Diethyl ether (DE) was used as the model compound of the PEO moiety of SEOS for simplicity. The electronic energies and structures of the stationary species of interest in the gas phase were calculated by full optimization without any geometrical constraints using the density functional theory method with Gaussian 03 software and Becke's three-parameter hybrid functional (B3LYP) [24] with a 6-31+g(d) basis set [25] for non-metallic elements and the effective core potential of the LANL2DZ basis [25] set for the iodide ion. The nature of all of the species was verified by calculating their vibrational frequencies [26,27]. The charge densities of the complexes were obtained using natural population analysis [28–30].

3. Results and discussion

3.1. Phase-change effect

Ion-gels were formed by the addition of 5 wt% of SEOS1 and SEOS2 to PMII, which can be seen in Fig. 1. It is known that the microphase separation of the solvatophobic styrene moiety at both ends of the SEOS copolymer cause the formation of a gel [19,20].

The WAXD was conducted to deduce the morphological information of SEOS films and PMII/SEOS1 and PMII/SEOS2 ion-gel electrolytes, and the results are shown in Fig. 2a and b, respectively.

The WAXD diffraction patterns of both the SEOS1 and SEOS2 films (Fig. 2a) showed two sharp peaks at 2θ = 18.3 and 22.4°, which are consistent with those of the crystalline PEO homopolymer [31].

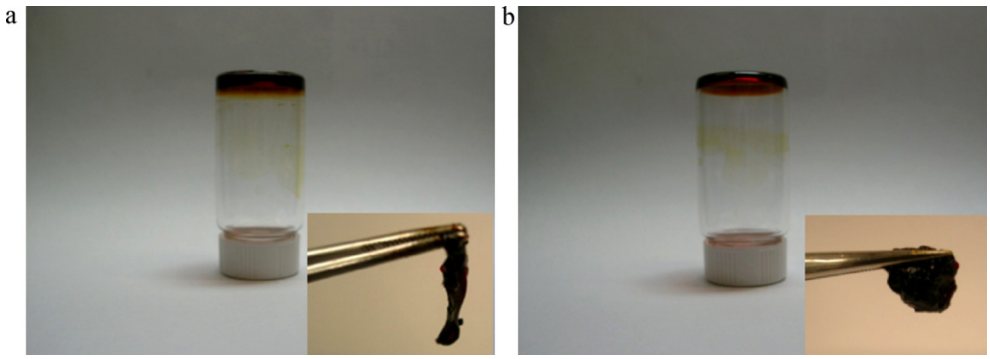

Fig. 1. The upside-down vessel containing the ion-gel formed with PMII and 5 wt% of (a) SEOS1 and (b) SEOS2 showing lack of fluidity of the system in this study.

This result shows that the polystyrene chains do not crystallize themselves or disturb the ordering of PEO in SEOS films [32].

Due to the interaction between the cation of PMII and oxygen of the ethylene oxide (EO) moiety of SEOS, there are no clear crystalline PEO peaks observed in the PMII/SEOS ion-gels, as shown in Fig. 2b. A broad peak is observed at $2\theta = 21.56^{\circ}$ for the ion-gel containing 5 wt% of SEOS1, implying the formation of a certain ordered structure inside the ion-gel. With the addition of SEOS2 to PMII, a broad amorphous halo is also observed at $2\theta = 23.65^{\circ}$, and the intensity increases with the addition of SEOS2.

Bragg d-spacings were calculated using Bragg's law and the peak maximum (i.e., $n\lambda = 2d\sin\theta$, where n is the positive integer, λ is the wavelength and θ is the angle), producing values of 0.41 and 0.38 nm for ion-gels containing SEOS1 and SEOS2, respectively. This distance corresponds to an intermolecular distance of the IL that would be dependent on the amount of PEO segment of SEOS.

The interaction between ionic species and polymeric ligands corresponds to a complexation (or dissociation in the inverse direction) process. Hence, related information such as complexation energy and/or structure can be predicted theoretically.

The interaction between EO and the imidazolium cation of PMII was calculated by an ab initio method. Two different stable conformers of PMII are possible, as shown in Fig. 3, i.e., iodide can be located in the plane or out of the plane created by the imidazolium ring. The conformer PMII(I) was slightly more stable than PMII(II) in the gas phase, but the Gibbs free energy difference between two conformers was ca. 0.67 kcal mol^{-1} (2.80 kJ mol^{-1}) at the B3LYP/6-31+g(d)/LANL2DZ level. Therefore, it is reasonable to expect that two conformers will be randomly distributed in a real system.

We chose DE as a model of the PEO moiety to consider the dissociation processes in only a singly coordinated structure for simplicity. The geometry of the PMII···DE complexes were optimized using the B3LYP/6-31+g(d)/LNAL2DZ method. All five initial configurations were constructed for geometry optimization. In the PMII(I)···DE complex, the O of DE was placed linearly along C2-H of the imidazolium phase (one horizontal, one vertical for the plane created by the imidazole ring) and one bottom of the imidazolium plane. For the PMII(II)···DE complex, the O of DE was placed on the top and bottom of the imidazolium plane. The optimized structures of the PMII···DE complexes with the most stable energy are shown in Fig. 3, which indicate that there are nonbonding

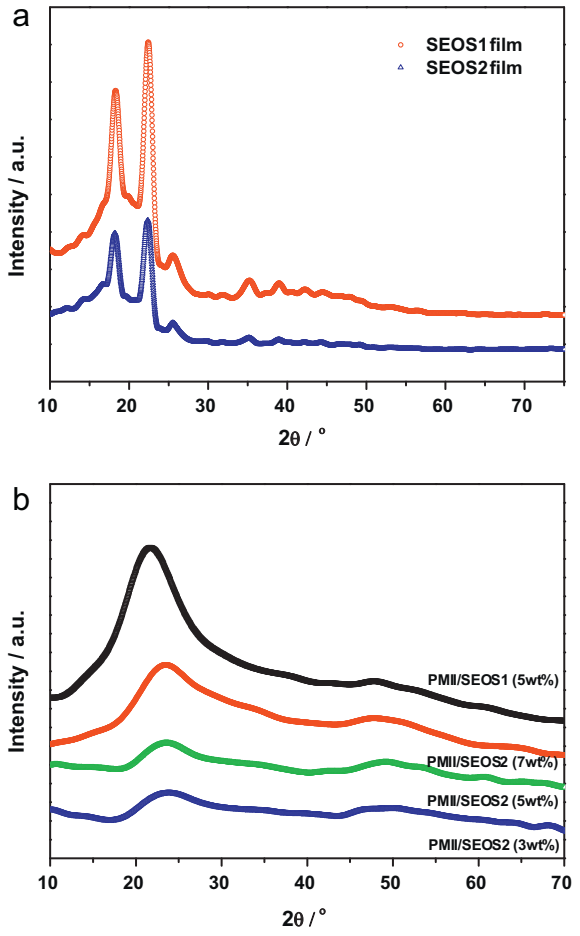

Fig. 2. WAXD curves for (a) SEOS1 and SEOS2 film and (b) ion-gels formed by 5 wt% SEOS1 and 3, 5, 7 wt% SEOS2 in PMII.

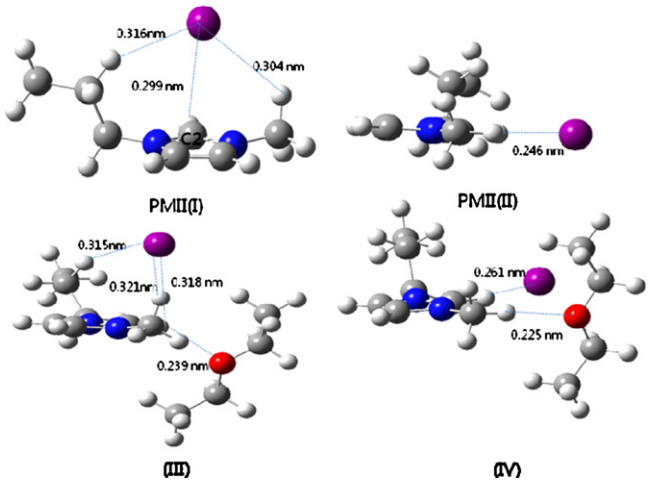

Fig. 3. Optimized structure of (a) PMII(I), (b) PMII(II) and the (c) complexes (III) and (d) (IV) formed between PMII(I) and PMII(II) with DE, respectively.

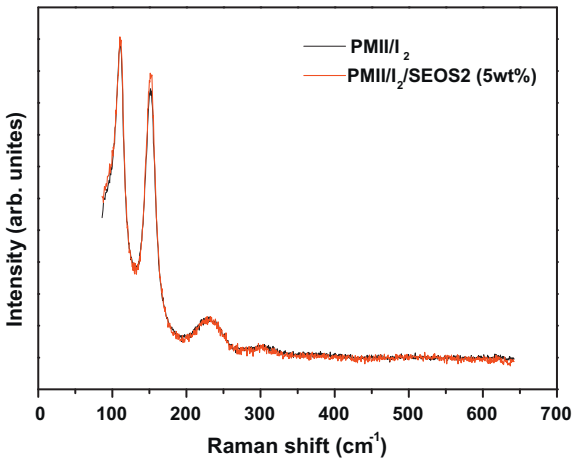

Fig. 4. Raman spectra of PMII/I_2 with and without the addition of 5 wt% of SEOS2.

interactions between the PMII and DE. The DE was coordinated vertically for the plane created by the imidazolium ring in complex (IV); however, it was tilted due to the stereo hindrance between DE and I^-, which are placed out of the plane of the imidazolium ring. The distance between dC2–H···O of DE was shorter for complex (IV) than that of complex (III). This difference resulted in a Gibbs free energy change for the formation of complex (IV) from PMII(II) and DE was more stable by 1.19 kcal mol^{-1} (4.98 kJ mol^{-1}) than that of complex (III) from PMII(I) and DE in the gas phase.

The charge densities of I^- changed from −0.816 and −0.835 to −0.831 and −0.854 for complex (III) and (IV), respectively, implying that the charge transfer is 0.015 and 0.019e, respectively. This theoretical study indicates that the PMII interacts with SEOS due to an ion–dipole interaction between the oxygen atoms in the EO and the imidazolium cations of PMII [21].

The optimized bond length between hydrogen attached to carbon (C2) and I^- (dC2–H···I) increased with the addition of DE. It increased from 0.299 to 0.318 nm for complex (III) and increased from 0.246 to 0.261 nm for complex (IV). The lengthening of the dC2–H···I complex compared to the one in PMII would improve the movement of I^- inside the quasi-solid matrix. It seems that the high concentration of loose I^- ions in the electrolyte due to the interaction between the oxygen atom of the EO units and the imidazolium cations [21] may help the mobility of the ions, resulting in high ionic conductivity.

The ionic conductivity values were 3.8 and 4.2×10^{-4} S cm^{-1} for PMII-based ion-gels containing 5 wt% SEOS1 and SEOS2 triblock copolymer, respectively, which are consistent with the value of PMII itself (5.8×10^{-4} S cm^{-1}) [33]. Moreover, the values are higher than those reported for polymer electrolytes based on PEO or poly(ethylene glycol) with ionic liquids ($\sim 1 \times 10^{-5}$ S cm^{-1}) [6]. The high ionic conductivity and the relatively low amount of polymer barrier inside of the ion-gel electrolyte, which allows for fast diffusion for dye regeneration, resulted in high cell performance.

We fabricated DSSCs using PMII-based electrolytes with and without SEOS. Because we intended to understand the effects of the solidification of the matrix by the formation of ion-gels in the DSSCs, the simple components of the electrolytes were fixed, i.e., PMII, I_2, and 1MB, which functions as a Lewis base. We adjusted the composition of PMII/I_2 to that reported in the literature [34], and the mole ratio of PMII/I_2/1MB was optimized to 12/0.5/1 in this study. The concentration of I^- was high in this system because the transport of I_3^- to the counter electrode is known to be a rate-limiting step in the viscous medium [35].

The chemical status was investigated by Raman spectroscopy. Fig. 4 shows the Raman spectra of the PMII/I_2 electrolyte with and without SEOS2. The triiodide symmetric stretching vibration is shown at 110 and 230 cm^{-1} [36]. Polyiodide (e.g., I_5^-) was also observed at 151 cm^{-1} in this system, which may be due to the high concentration of I_2 in this electrolyte system. The intensity and the position of the line did not change with the addition of SEOS2 in the PMII/I_2 electrolyte, implying a negligible effect.

Because the interfacial contact between dye-adsorbed semiconductor nanoparticles and electrolytes is a major factor in determining the electron transfer efficiency and, consequently, the overall conversion efficiency for the case of a non-liquid phase, the penetration of ion-gel electrolytes into the pores of a semiconductor layer must be maximized to promote interfacial contact between the electrolyte and the dye. SEM photomicrographs of the cross-sections of a DSSC employing ion-gels are shown in Fig. 5. The cross-sectional images of the nanoparticles are indistinct in the presence of an ion-gel. This is due to the good contact between the dye-adsorbed TiO_2 particles and the ion-gel electrolyte.

The photovoltaic performances of DSSCs under AM 1.5 irradiation (100 mW cm^{-2}) with masking and a non-reflecting black layer under the cell are shown in Fig. 6. The wt% of SEOS triblock polymer was fixed to 5 wt%. The characteristic photovoltaic parameters including the short-circuit current density (J_{sc}), open-circuit voltage (V_{oc}), fill factor (FF), and photovoltaic conversion efficiency (η) are listed in Table 1. The photovoltaic parameters of the DSSCs containing PMII/I_2/1MB electrolyte were 5.19 mA cm^{-2}, 0.60 V, 67.97 and 2.21%, respectively, for the reference without SEOS; these values are lower than those reported in the literature [34] due to the simplified component and the different choice of dye and additives in this research.

In general, the photovoltaic performance of DSSCs composed of PMII electrolyte is low due to the significant recombination of injected electrons with an oxidized mediator present in the electrolyte at the surface of TiO_2 semiconductor particles [37] and the quenching of excited sensitizers due to the high concentration of iodide [38]. The use of a high concentration of I^- in this electrolyte system to avoid the mass transport limitation of I_3^- [34] caused an enhancement in the rate of reductive quenching of the excited sensitizer, creating another channel for deactivation and resulting in the loss of a significant amount of the potential photocurrent [34].

Changing liquid-state IL to a quasi-solid ion-gel maintained and/or increased in J_{sc}. While J_{sc} increased from 5.19 to 5.72 and 5.84 mA cm^{-2}, η increased from 2.21 into 2.54 and 2.63% for the DSSCs containing electrolytes with 5 wt% SEOS1 and SEOS2, respectively. In general, the photovoltaic characteristic parameters were reduced after the electrolyte state was solidified. It is important to note that the increase in J_{sc} and the conversion efficiency in this study are remarkable with respect to the phase change of the electrolyte from a liquid to a gel state.

The electrochemical impedance spectroscopy (EIS) spectra support the photovoltaic performance of the DSSCs. Fig. 7 shows Nyquist plots of the DSSCs, and the corresponding electrochemical parameters were obtained by fitting the plots using the equivalent circuit shown in the insert.

The three semicircular shapes are assigned to impedances related to charge transport at the Pt electrode, at the TiO_2/dye/electrolyte interface and diffusion within the electrolyte, respectively [39]. It is noted that the first semicircle slightly increased with the addition of the SEOSs, and the corresponding charge-transfer resistance (R_1) slightly increased, implying that the activation barrier for electron transfer from the Pt electrode to I_3^- increases as a result of the interaction between the iodide (including polyiodide) and SEOSs; however, the increase is very small. Meanwhile, the charge-transfer resistance at the TiO_2/dye/electrolyte interface also increased with the addition of the SEOSs, implying a decrease in recombination due to the formation of the I^-···SEOS complex. Compared with the performance of

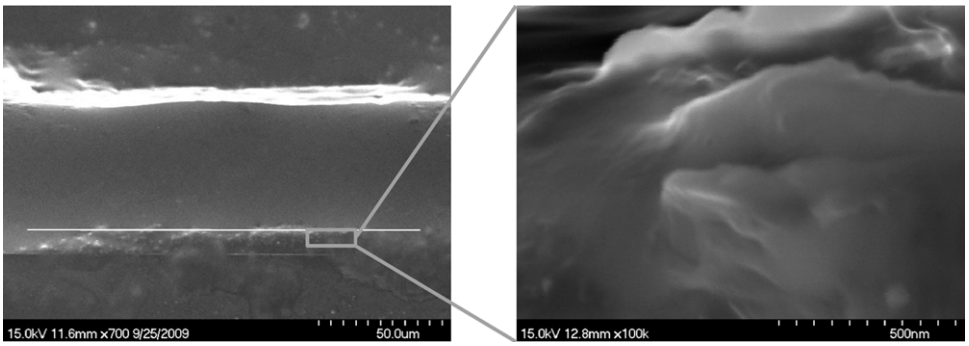

Fig. 5. Cross-sectional SEM image of DSSCs with PMII ion-gel electrolyte containing 5 wt% SEOS2.

Table 1
Photovoltaic performance of DSSCs with the ion-gel electrolyte PMII containing 5 wt% SEOS 1 and SEOS2.

	V_{oc} (V)	J_{sc} (mA cm^{-2})	Fill factor	Efficiency (%)	R_1 (Ω)	R_2 (Ω)	Lifetime (ms)
Reference	0.60	5.19	67.97	2.21	7.23	8.42	4.45
SEOS1	0.62	5.72	68.69	2.54	8.42	12.7	7.02
SEOS2	0.65	5.84	71.23	2.63	9.43	16.8	10.05

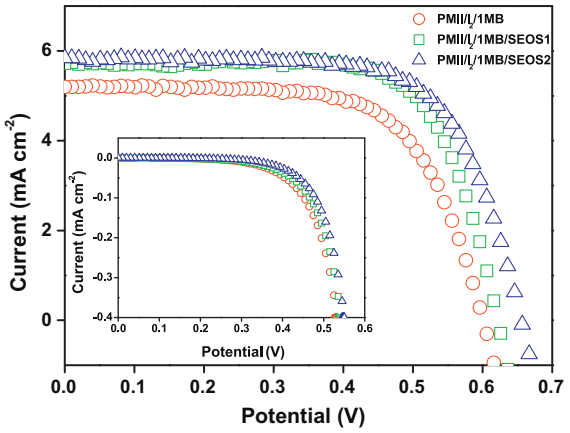

Fig. 6. Photocurrent density–potential characteristics of DSSC assembled with PMII ion-gel electrolyte containing 5 wt% SEOS 1 and SEOS2 under 100-mW cm^{-2} irradiation.

the reference DSSC, we found that the charge-transfer resistance and the electron lifetime (τ), which was determined by the product of R_1 and CPE2, increased in the ion-gel due to the retardation of electron recombination by I_3^- on the TiO_2 surface. This can also be observed in the *J–V* curve measured in the dark shown in Fig. 6. Although it does not reflect the exact circumstances of recombination under illumination, the dark current can be used as an estimate of the extent of reduction of I_3^- by conduction-band electrons. The onset voltage of the cells increased with the use of the ion-gel, which was significant for the ion-gel composed of SEOS2 under the same conditions. This result suggests that the substitution of the liquid phase of PMII into the quasi-solid phase of the ion-gel electrolyte is effective in retarding the back reaction. Thus, it is concluded that the increased charge-transfer resistance at the Pt/electrode and the reduced recombination explain the complementary cooperation effect on the photovoltaic performance of DSSCs containing a quasi-solid electrolyte.

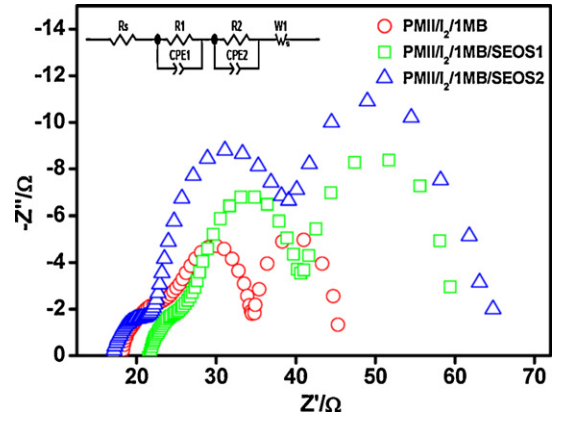

Fig. 7. Nyquist plot of DSSCs with PMII ion-gel electrolyte containing 5 wt% SEOS1 and SEOS2 measured in the dark. The equivalent circuit of this study is shown in the insert.

The long-term stability of DSSCs assembled using a PMII electrolyte and with and without SEOS2 (5 wt%) was evaluated. Fig. 8 compares the variation in J_{sc} and η of the DSSCs as a function of time. Both J_{sc} and η in DSSCs containing liquid-state PMII decayed with time; the values decreased to 27.5% and 22% of their initial value after 1440 h, respectively, while both values decreased to 13.5% and 8% of their initial values, respectively, for the DSSCs containing SEOS2, indicating the improved long-term stability of DSSCs containing ion-gel electrolytes.

3.2. Barrier effect

One method to improve the photovoltaic performance by reducing recombination is to create a barrier by the surface modification of TiO_2 semiconductor nanoparticles using a well-defined structural material such as dendron. The barrier effect of dendrons was tested in this system using fifth generation (G5) dendrons possessing a carboxylic acid group at its center [22]. The average pore diameter and the surface area of the TiO_2 film were 15.8 nm and 123.2 m^2 g^{-1}, respectively, as determined by the Brunauer–Emmett–Teller method from the Ar desorption isotherm [40]; the end-to-end distance of G5 dendron was estimated to be 2.9 nm [22]. Therefore, dendron preferentially penetrated into the mesopores of the TiO_2 layers, resulting in an increased interfacial coverage of the TiO_2 bare surface.

The photovoltaic performance of DSSCs with dendron are shown in Fig. 9 and Table 2. The mole number of dendrons was fixed at 5.17×10^{18} moles per gram (TiO_2). The surface coverage of the TiO_2 particle was roughly estimated to be 14% under the assumption of homogeneous adsorption of dendrons in TiO_2 film without N719.

Table 2
Photovoltaic performance of DSSCs with the ion-gel electrolyte PMII containing 5 wt% SEOS 1 and SEOS2 after dendron treatment.

	V_{oc} (V)	J_{sc} (mA cm^{-2})	Fill factor	Efficiency (%)	R_1 (Ω)	R_2 (Ω)	Lifetime (ms)
Reference	0.61	6.52	68.79	2.74	16.92	112.1	7.96
SEOS1	0.63	6.73	71.75	3.04	26.46	148.6	9.36
SEOS2	0.65	7.16	72.26	3.34	40.31	229.5	11.02

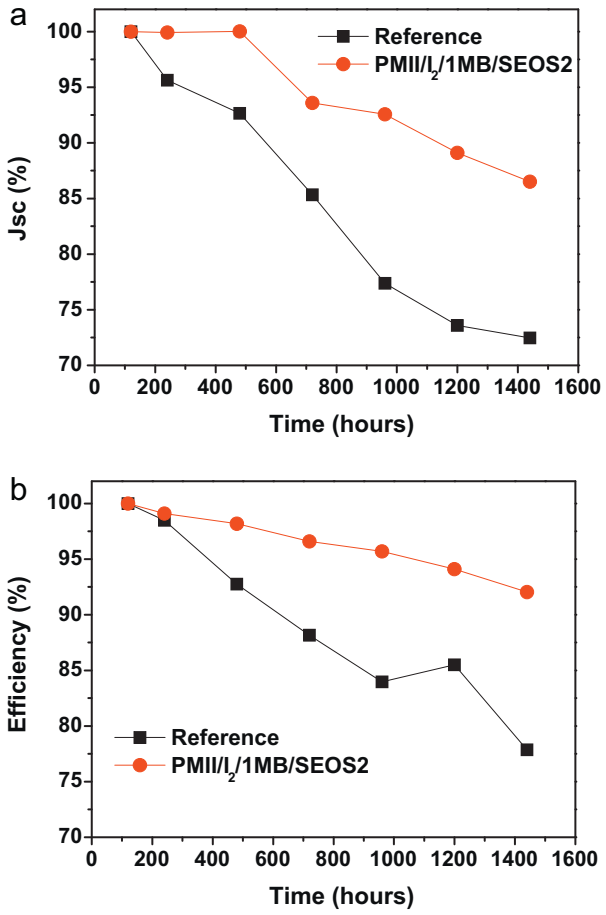

Fig. 8. Variation of (a) short-circuit current density and (b) conversion efficiency as a function of time for the DSSCs assembled using PMII electrolyte with and without SEOS2 (Active area of the cells were 0.4 cm × 0.4 cm).

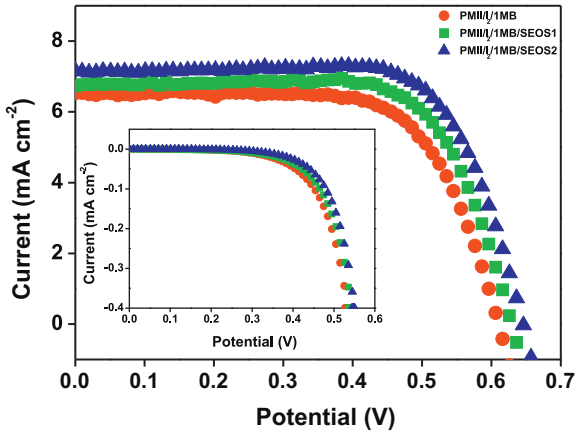

Fig. 9. Photocurrent density-potential characteristics of DSSCs assembled with PMII ion-gel electrolyte containing 5 wt% SEOS1 and SEOS2 with dendron treatment under 100 mW cm^{-2} irradiation.

All DSSC systems showed an improvement in J_{sc} and η upon the addition of G5 dendron co-adsorbents.

The electron transfer from the conduction band of the mesoscopic TiO_2 film to the I_3^- ions in the electrolyte was measured by EIS in the dark and is represented by the semi-circles shown in Fig. 10. Analyzing EIS using an appropriate equivalent circuit model yielded the parameters of charge-transfer resistance R_2 corresponding to the recombination current across the TiO_2/electrolyte interface.

The Nyquist plot shows that the R_2 increased for the DSSCs containing ion-gels, meaning that the charge recombination between the injected electrons and the electron acceptors in the redox electrolyte, I_3^-, was retarded significantly with the addition of dendron. The increase in the electron lifetime in the ion-gel due to the retardation of electron recombination with I_3^- on the TiO_2 surface indicates that the addition of dendrons decreases the interfacial rate constant for electrons captured by the I_3^- ions. The increase in the recombination lifetime in the TiO_2 film is associated with a rise in the charge-transfer resistance, indicating that the transformation of the matrix into a gel as well as the addition of dendron decreases the interfacial rate constant for electron capture by the I_3^- ions. That is, the presence of dendron effectively forms a barrier layer that blocks the recapture of the electron photo-injected by I_3^-, resulting in a higher charge collection efficiency.

One interesting observation in this study was the increase in J_{sc} in the DSSCs with the ion-gel electrolyte, which was confirmed by IPCE measurements. The IPCE value represents the conversion efficiency of incident photon to current, the cell clearly exhibited an impressive response over the entire region compared to the reference cells, as indicated by the IPCE data shown in Fig. 11. Because the carboxylic acid moieties of the dendrons were bound to oxide surfaces [41], the added dendrons would produced a more compact monolayer than that formed when the sensitizer was adsorbed alone. The attached dendron also eliminated most of the hydrophilic surface sites that were available for water absorptions, which reduced the cell efficiency. It is known that the value of J_{sc} depends on the amount of sensitizer adsorbed to the TiO_2 nanoparticles and the optimal sensitizer conformation. Because the concentration of the sensitizer in this system was fixed, the increase

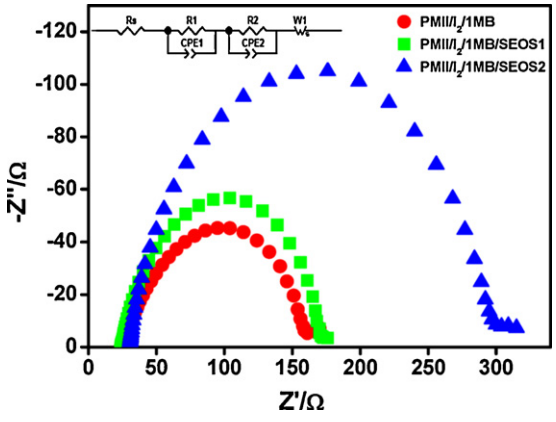

Fig. 10. Nyquist plot of DSSCs with PMII ion-gel electrolyte containing 5 wt% SEOS1 and SEOS2 after Dendron treatment. The equivalent circuit of this study is shown in the insert.

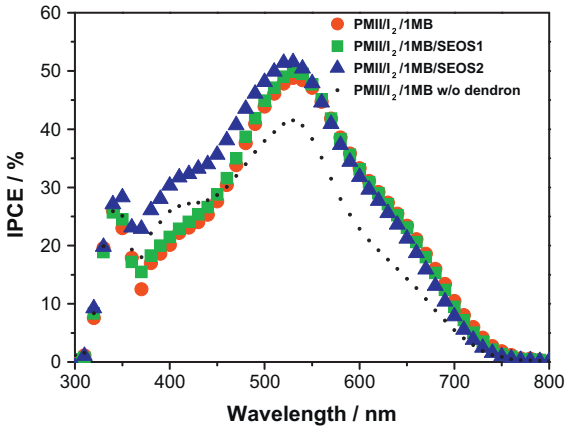

Fig. 11. IPCE spectra of DSSCs with PMII ion-gel electrolyte containing 5 wt% SEOS 1 and SEOS2 with and without the addition of dendron.

in the J_{sc} may have been due to the retarded interfacial charge recombination dynamics [42], and optimized conformation.

In conclusion, we have demonstrated that quasi-solid ion-gel electrolytes consisting of small amounts of SEOS triblock copolymer in PMII provide improved DSSC performance over DSSCs using ionic liquid electrolytes. To our knowledge, this is the first time both J_{sc} and η have been increased by simply changing the phase of the electrolyte in DSSCs. From the long-term stability results, it is expected that the ion-gel state DSSC is a promising solar cell that exhibits good durability. In addition, up to a 27% increase in the total power conversion efficiency was achieved with G5 dendron as the co-adsorbent due to the suppression of surface recombination and the surface coverage of the TiO_2 particles.

Acknowledgements

This work was supported by the Basic Science Research Program through the National Research Foundation of Korea (NRF) funded by the Ministry of Education, Science and Technology of Korea (No. 2010-0020918) and for the center for Next Generation Dye-sensitized Solar Cells (No. 2011-0001055).

References

[1] Y. Chiba, A. Islam, Y. Watanabe, R. Komiya, N. Koide, L. Han, Jpn. J. Appl. Phys. 45 (2006) L638–L640.
[2] R.H. Baker, S.M. Zakeeruddin, S. Ito, P. Liska, R. Charvet, P. Comte, M.K. Nazeeruddin, P. Pechy, M. Takata, H. Miura, S. Uchida, M. Grätzel, Adv. Mater. 18 (2006) 1202–1205.
[3] U. Bach, D. Lupo, P. Comte, J.E. Moser, F. Weissörtel, J. Salbeck, H. Spreitzer, M. Grätzel, Nature 395 (1998) 583–585.
[4] P. Wang, S.M. Zakeeruddin, J.-E. Moser, R.H. Baker, M. Grätzel, J. Am. Chem. Soc. 126 (2004) 7164–7165.
[5] J.H. Kim, M.S. Kang, Y.J. Kim, J. Won, N.G. Park, Y.S. Kang, Chem. Commun. (2004) 1662–1663.
[6] J.H. Kim, Y.J. Kim, M.-S. Kang, M.J. Lee, J. Won, J.C. Lee, Y.S. Kang, Adv. Mater. 16 (2004) 1753–1757.
[7] M.S. Kang, J.H. Kim, Y.J. Kim, J. Won, N.G. Park, Y.S. Kang, Chem. Commun. (2005) 889–891.
[8] J.H. Kim, M.S. Kang, J. Won, Y.S. Kang, J. Photochem. Photobiol. A: Chem. 183 (2006) 15–21.
[9] A.F. Nogueira, J.R. Durrant, M.A. De Paoli, Adv. Mater. 13 (2001) 826–830.
[10] T. Stergiopoulos, A.M. Arabatzis, G. Katsaros, P. Falaras, Nano Lett. 2 (2002) 1259–1261.
[11] W. Kubo, T. Kitamura, K. Hanabusa, Y. Wada, S. Yanagida, Chem. Commun. (2002) 374–375.
[12] S.M. Zakeeruddin, P. Wang, I. Exnar, M. Grätzel, Chem. Commun. (2002) 2972–2973.
[13] P. Lianos, E. Stathatos, U.L. Stangar, B. Orel, Adv. Mater. 14 (2002) 354–358.
[14] D. Lupo, U. Bach, P. Comte, J.E. Moser, F. Weissortel, J. Salbeck, H. Spreitzer, M. Gratzel, Nature 395 (1998) 583–585.
[15] C.J. Brabec, D. Gebeyehu, N.S. Sariciftci, D. Vangeneugden, R. Kiebooms, D. Vanderzande, F. Kienberger, H. Schindler, Synth. Met. 125 (2002) 279–287.
[16] S.K.T. Nakade, Y. Wada, S. Yanagida, Langmuir 21 (2005) 10803–10807.
[17] J.N. De Freitas, A.F. Nogueira, M.-A. De Paoli, J. Mater. Chem. 19 (2009) 5279–5294.
[18] A.F. Nogueira, C. Longo, M.-A. De Paoli, Coord. Chem. Rev. 248 (2004) 1455–1468.
[19] M. Watanabe, T. Ueki, Macromolecules 41 (2008) 3739–3749.
[20] B.D. Cahan, J.S. Wainright, J. Elec. Chem. 140 (1993) L185–L186.
[21] P.G.B.Y. He, P. Bühlmann, T.P. Lodge, J. Phys. Chem. B 111 (2007) 4645–4652.
[22] B. Shin, J. Won, T. Son, Y.S. Kang, C.K. Kim, Chem. Commun. 47 (2011) 1734–1736.
[23] T.P. Lodge, Y. He, Macromolecules 41 (2008) 167–174.
[24] A.D. Becke, J. Chem. Phys. 98 (1993) 5648.
[25] W.J. Hehre, L. Radom, P.V.R. Schleyer, J.A. Pople, Ab Initio Molecular Orbital Theory, John Wiley & Sons, New York, 1986, 548 p.
[26] J.A. Pople, R. Krishnan, H.B. Schlegel, J.S. Binkley, Int. J. Quantum Chem. 13 (1979) 225.
[27] J.A. Pople, H.B. Schlegel, R. Krishnan, D.J. Defrees, J.S. Binkley, M.J. Frisch, R.A. Whiteside, R.F. Hout, W.J. Hehre, Int. J. Quantum Chem. 15 (1981) 269.
[28] S. Miertus, E. Scrocco, J. Tomasi, Chem. Phys. 55 (1981) 117.
[29] V. Barone, M. Cossi, J. Phys. Chem. A 102 (1998) 1995.
[30] M. Cossi, V. Barone, J. Phys. Chem. A 104 (2000) 10614.
[31] Y. He, P.G. Boswell, P. Buhlmann, T.P. Lodge, J. Phys. Chem. B 111 (2007) 4645–4652.
[32] J. Xi, X. Qiu, W. Zhu, X. Tang, Micropor. Mesopor. Mater. 88 (2006) 1–7.
[33] D.M. Zu, K. Zhang, J.-F. Wu, J. Appl. Polym. Sci. 101 (2006) 727–730.
[34] Y. Bai, Y. Cao, J. Zhang, M. Wang, R. Li, P. Wang, S.M. Zakeeruddin, M. Grätzel, Nat. Mater. 7 (2008) 626–630.
[35] F.S. Freitas, J.N. de Freitas, B.I. Ito, M.-A. De Paoli, A.F. Nogueira, ACS Appl. Mater. Interfaces 1 (2009) 2870–2877.
[36] P. Deplano, J.R. Ferraro, M.L. Mercuri, E.F. Trogu, Coord. Chem. Rev. 188 (1999) 71–95.
[37] N. Papageorgiou, P.P. Infelta, M. Gratzel, J. Phys. Chem. B 102 (1998) 4156–4164.
[38] P. Wang, J. Am. Chem. Soc. 127 (2005) 6850–6856.
[39] A. Hagfeldt, G. Boschloo, Acc. Chem. Res. 42 (2009) 1819–1826.
[40] S. Brunaure, P. Emmett, E. Teller, J. Am. Chem. Soc. 60 (1938) 309.
[41] K. Dobson, A. Mcquillan, Spectrochim. Acta A 56 (2000) 557.
[42] F. Gao, Y. Wang, D. Shi, J. Zhang, M. Wang, X. Zing, R.H. Baker, P. Wang, S.M. Zakeeruddin, M. Gratzel, J. Am. Chem. Soc. 130 (2008) 10720–10728.